Development of a synergistic damage mechanics model to predict evolution of ply cracking and stiffness changes in multidirectional composite laminates under creep

Thomas Berton, John Montesano and Chandra Veer Singh

Abstract

A physics-based multi-scale model that couples viscoelasticity and time-dependent damage evolution for general multidirectional laminates subjected to long-term creep loading is developed. The viscoelastic ply behavior is evaluated using a nonlinear Schapery-type viscoelastic model, while a methodology employed within the framework of classical laminate theory is used to predict the corresponding laminate time-dependent response. The evolution of microscopic ply cracks in multiple plies with different orientations during creep loading is predicted using an energy-based approach, and the corresponding laminate stiffness degradation is evaluated using a synergistic damage mechanics-based model that relies on computational micromechanics in lieu of costly experimental data. The developed model is used to predict the evolution of ply cracks and the viscoelastic stress–strain response of various cross-ply and multidirectional laminates under quasi-static and creep loading. Predicted strains, compliance changes and crack density evolutions show excellent agreement with available experimental creep data for different laminate stacking sequences, providing validation for the model. Predictions are also made for two additional multidirectional laminates in order to investigate the effect of off-axis ply angle on the creep response, which demonstrates the versatility of the model and its usefulness in assessing the long-term durability of general multidirectional composite laminates.

Keywords

Multidirectional laminates, damage evolution, stiffness degradation, viscoelasticity, creep loading, computational micromechanics

Materials Science and Engineering, University of Toronto, Toronto, Canada

Corresponding author:
Chandra Veer Singh, Materials Science and Engineering, University of Toronto, 184 College St., Suite 140, Toronto, ON, M5S 3E4, Canada.
Email: chandraveer.singh@utoronto.ca

Introduction

The design of high performance composites requires an understanding of damage evolution and its effects on mechanical property degradation, which enables the prediction of their durability and damage tolerance properties. Several models based on the shear-lag principle (Lim and Hong, 1989), variational analysis (Hashin, 1987) or multi-scale synergistic damage mechanics (SDM; Talreja and Singh, 2012) have previously been developed for predicting damage evolution and performance degradation in linearly elastic laminated composites. Among these, the models based on shear-lag and variational principles make certain approximations that reduce the dimensionality of the physical problem, which limits their applicability to simple laminate configurations such as cross-ply laminates. The SDM-based model (Talreja and Singh, 2012) combines computational micro-damage mechanics with continuum damage mechanics (CDM) for evaluating the corresponding elastic stiffness degradation in multidirectional laminates, eliminating the need for costly experimental test data, a key limitation in traditional CDM approaches (Talreja, 1985). In addition, analytical solutions to complicated boundary value problems for multidirectional laminates with multiple modes of damage are avoided when using the SDM-based model, which is a drawback for the shear-lag and variational approaches. The SDM-based model is suitable for general multidirectional laminates with multiple modes of damage, including cross-ply, angle-ply (Singh and Talreja, 2008) and quasi-isotropic laminates (Singh and Talreja, 2009) subjected to general in-plane multiaxial loading (Montesano and Singh, 2015a).

Although laminates generally exhibit linear elastic deformation behaviour, viscoelasticity may be an important characteristic for laminates exposed to high temperatures or subjected to matrix-dominated loading conditions. Other material systems, such as novel bio-composites, may be even more prone to time-dependent behaviour. Viscoelastic models that predict the response of laminates subjected to quasi-static and creep loads typically utilize Schapery's constitutive relationships (Lévesque et al., 2008; Rozite et al., 2011; Schapery, 1969). These models are based on a continuum thermodynamic framework, where a general methodology for empirical calibration of the model parameters is provided by Lévesque et al. (2008). However, current models that account for both damage evolution and the time-dependent response of laminates have significant shortcomings, which limit their applicability for predicting the long-term response of general multidirectional laminates. In an earlier report, Varna et al. (2004) extended the SDM approach by quantifying the time-dependent crack opening displacements (CODs) of transverse ply cracks in cross-ply laminates undergoing creep loading using a micromechanical finite element (FE) model. The FE model was used to calibrate the damage model, and the degradation of laminate properties under a fixed state of damage was predicted. Although the model accurately predicts time-dependent compliance increase when compared to independent FE micromechanical simulations, it has not been validated with experimental data, and the evolution of cracking is not considered. Moreover, the model is only valid for linearly viscoelastic cross-ply laminates, and the evaluation of the CODs requires a time-dependent nonlinear solution, which is computationally expensive. Ahci and Talreja (2006) developed a CDM-based model to predict the degradation of elastic and nonlinear viscoelastic properties for laminates under a fixed state of damage. This model, however, requires experimental data for calibration, does not consider damage evolution and is restricted in application to cross-ply laminates.

In regards to rate-dependent damage progression in laminates, Nguyen and Gamby (2007) studied crack density evolution in cross-ply laminates subjected to quasi-static loading under different applied strain rates. Through experiments, they found an increase in crack density evolution for higher applied strain rates and developed a shear-lag model with a rate-dependent
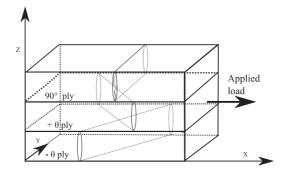
fracture criterion to predict the observed damage evolution. In this work, performance degradation was not predicted, and the analysis was restricted to cross-ply laminates, where the extension to more complex stacking sequences would be a challenge due to the complexity of the shear-lag model used. Asadi and Raghavan (2011) studied the behaviour of a $[\pm45/90_2]_s$ laminate undergoing creep at different applied loads. They measured crack density evolution during several creep tests as well as the stiffness degradation for different states of damage. Polynomial expressions used to fit the empirical data were required to calibrate the proposed model, which predicted damage evolution and the laminate viscoelastic response under creep loading. Asadi (2013) later provided a mathematical basis for their previous experimental results using a variational approach. The developed analytical model evaluated the stresses and strains in the laminate plies, and an energy-based fracture criterion was used to determine crack density evolution and the corresponding stress–strain behaviour. Although the prediction results correlate well with the obtained experimental data, mathematically the model is highly complex and it only applies to a particular stacking sequence (viz. $[\pm45/90_2]_s$); its extension to other configurations is not straightforward and has not been discussed.

Based on the cited literature, it is clear that comprehensive physics-based models capable of predicting the long-term behaviour of laminates, that consider both the viscoelastic response and the effect of time- or rate-dependent damage evolution, are currently lacking. Therefore, the aim of this study is to develop a physics-based multi-scale prediction model for general laminates subjected to long-term creep loading in order to address this gap. The proposed model is capable of predicting the evolution of subcritical ply cracks in multidirectional laminates by using an energy-based approach, where computational micromechanics is used in an SDM framework to calibrate the laminate constitutive equations for predicting the corresponding laminate property degradation. The coupled time-dependent ply response is evaluated using a nonlinear Schapery-type viscoelastic model, which allows for prediction of the associated laminate deformation response under creep loading. Details of the developed model and the overall predictive methodology are provided in the subsequent section.

Model description

Consider a multidirectional viscoelastic laminate loaded quasi-statically in uniaxial tension. At a critical load, the off-axis plies begin to develop unstable matrix cracks which quickly grow parallel to the fibre directions and through the lamina thickness, eventually resting at the ply interfaces (see Figure 1). This progressive damage although will not cause immediate failure, but will lead to appreciable laminate stiffness degradation. The SDM model developed in our previous work (Singh and Talreja, 2009) solves the problem of stiffness degradation for multidirectional linear elastic laminates using micro-damage mechanics to quantify the effect of matrix micro-cracks on laminate compliance, thus bypassing the need for experimental testing or complex and approximate analytical formulations. This model has recently been extended to the case of multiaxial loading conditions (Montesano and Singh, 2015a) and has been successfully combined with an accurate damage evolution model for cross-ply and multidirectional laminates under biaxial loading conditions (Montesano and Singh, 2015b, 2015c), thus allowing for a full prediction of the quasi-static deformation response of multidirectional laminates under multiaxial loading states.

Nevertheless, no model currently exists that can account for progressive damage development in multidirectional laminates under viscoelastic deformation. In the case of creep loading, cracks will open up with time progressively, which will affect crack density evolution as well as

Figure 1. Schematic showing multiple damage modes in a multidirectional symmetric laminate loaded axially. Cracks are assumed to extend parallel to the fibres throughout the laminate's width and through the laminate thickness.

performance degradation in a complex fashion. In the current study, the SDM approach is extended to account for the effects of viscoelasticity on damage evolution and performance degradation during creep loading. The time-dependent ply crack density evolution and the increase in compliance due to both creep and damage are predicted, and the long-term laminate creep response is evaluated.

For the sake of completeness, we briefly summarize the SDM model for the elastic case. The details of this model can be found in Talreja (1994), Singh and Talreja (2008) and Talreja and Singh (2012) Next, we will describe the energy-based model for predicting crack density evolution under elastic and viscoelastic conditions. Subsequently, we extend the SDM model to the viscoelastic case by combining it with a nonlinear Schapery-type model.
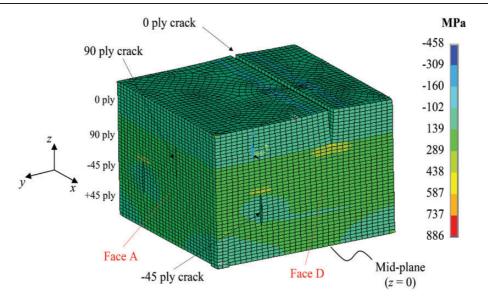
Laminate stiffness degradation and damage evolution

The damage state for ply cracking damage mode α in a multidirectional laminate can be described using a second-order tensor (Talreja, 1994)

$$D_{ij}^{(\alpha)} = \frac{\kappa_\alpha t_\alpha^2}{s_\alpha t} n_i n_j \tag{1}$$

The mode of damage α refers to the orientation of the cracks, which depends on the orientation of the layers in which the cracks extend (see Figure 1). In the equation above, κ_α is a constraining parameter that accounts for the effect of stacking sequence and crack density for the COD of the specific damage mode α (i.e. the constraining effect on COD by the adjacent layers as shown in Figure 2). Note that in general, the constraint parameters can include the effects of the adjacent viscoelastic plies. The parameters t_α and s_α are respectively the cracked ply thickness and the spacing between cracks, t is the total laminate thickness and n_i are unit vectors that define the crack surface orientation.

The damage tensor defined by equation (1) can now be used to evaluate the stiffness tensor for the laminate following the process described in Singh and Talreja (2009). For a general thin symmetric orthotropic laminate containing multidirectional damage in the form of ply cracks, the stiffness

Figure 2. FE representative unit cell for a $[0/90/\pm45]_s$ laminate containing ply cracks in the 90°, 0° and 45° plies. This model is used to calibrate the laminate stiffness tensor using evaluated CODs as well as the energy release rate for crack multiplication. COD: crack opening displacement; FE: finite element.

tensor is defined as (Montesano and Singh 2015a)

$$
C_{pq} = \begin{pmatrix} \frac{E_x^0}{1-\nu_{xy}^0\nu_{yx}^0} & \frac{\nu_{xy}^0 E_y^0}{1-\nu_{xy}^0\nu_{yx}^0} & 0 \\ \frac{\nu_{xy}^0 E_y^0}{1-\nu_{xy}^0\nu_{yx}^0} & \frac{E_y^0}{1-\nu_{xy}^0\nu_{yx}^0} & 0 \\ 0 & 0 & G_{xy}^0 \end{pmatrix} - \sum_\alpha a_\alpha D_\alpha \begin{pmatrix} 2a_1^{(\alpha)} & a_4^{(\alpha)} & 0 \\ a_4^{(\alpha)} & 2a_2^{(\alpha)} & 0 \\ 0 & 0 & 2a_3^{(\alpha)} \end{pmatrix} \tag{2}
$$

In the above equation, the first term on the right-hand side is the stiffness tensor for a pristine linear elastic laminate, which can be evaluated using classical laminate theory (CLT). The second term is the contribution of all the damage modes on the stiffness degradation. It should be noted that the stiffness tensor defined by equation (2) does not include the viscoelastic effects of the plies – this will be discussed in the subsequent sections. The factor D_α is related to the COD through κ_α and is based on the damage tensor terms defined by equation (1). The $a_i^{(\alpha)}$ terms are the laminate damage constants, which describe the loss in stiffness due to matrix micro-cracking for a given damage mode α. The $a_i^{(\alpha)}$ terms in equation (2), as well as the constraint parameters κ_α in equation (1), are obtained herein from FE computational micro-damage models for a particular laminate group (see Montesano and Singh, 2015a for definition of representative volume elements (RVEs) and accompanying boundary conditions for analyzing ply cracking in multiple orientations). These models are used to directly evaluate the CODs for particular damage modes under various crack densities, the details of which are described by Singh and Talreja (2009) and Montesano and Singh (2015a).

As indicated, an energy-based approach is used here to predict ply crack density evolution in a laminate, which also utilizes the CODs evaluated from the FE micro-damage mechanics models (see Singh and Talreja, 2010 and Montesano and Singh, 2015b). The energy release rate, required to

form additional cracks during a crack multiplicative process is evaluated using the following expression

$$W_I = \frac{(\sigma_2^\alpha)^2 t_\alpha}{E_2}\left[2\tilde{u}_n^\alpha\left(\frac{s_\alpha}{2}\right) - \tilde{u}_n^\alpha(s_\alpha)\right] \tag{3}$$

where σ_2^α is the far-field transverse stress driving crack opening, E_2 is the virgin transverse stiffness of the ply and $\tilde{u}_n^\alpha$ is the normalized COD for the indicated crack spacing. It should be noted that E_2 is in fact a function of time, allowing the changing ply stiffness caused by viscoelasticity to be considered during ply crack evolution. For a given damage mode of a multidirectional laminate for a prescribed loading condition, ply crack multiplication occurs when W_I is larger than the critical energy release rate G_{Ic}. The critical energy release rate G_{Ic} is evaluated using a numerical technique based on the virtual crack closure technique in lieu of fitting empirical data, where similar FE computational micro-damage models are used. The developed model also accounts for the stochastic nature of the ply crack evolution process through a two-parameter Weibull distribution for G_{Ic} (see Montesano and Singh, 2015b).

Viscoelasticity and creep

The laminate constitutive equations presented in the previous section are extended to account for the time-dependent laminate behaviour using the ply viscoelastic properties. Previous studies have shown that glass-fibre and carbon-fibre epoxy plies exhibit creep behaviour mainly in the transverse and shear directions during extended periods of loading (Asadi and Raghavan, 2011; Nguyen and Gamby, 2007). In order to define the time-dependent creep compliance tensor terms for a single ply, a modified Kohlrausch–Williams–Watts (KWW) model is used in this study and is defined by Asadi and Raghavan (2011) for the transverse and shear components of the compliance tensor:

$$S_{ii,\text{creep}}(t) = g_{ii}^{(0)}S_{ii}^{(0)} + g_{ii}^{(1)}g_{ii}^{(2)}\Delta S_{ii}\left(1 - \exp\left(-\left[\left(\frac{t}{a_\sigma\tau}\right)^c\right]\right)\right) \quad (i = 2,6) \tag{4}$$

Here, $S_{ii}^{(0)}$ denotes the instantaneous elastic ply compliance; $g_{ii}^{(0)}$ represents a nonlinear, stress-dependent parameter accounting for the increase in compliance at higher stresses; $g_{ii}^{(1)}$ and $g_{ii}^{(2)}$ are nonlinear, stress-dependent parameters accounting for the increase in the time-dependent compliance $\Delta S_{ii}(t)$, with t describing time; and a_σ, τ and c are data-fitting ply constants, with τ the time constant describing the rate of change in compliance with time.

In general, a Schapery-type model can be applied to a variety of composite materials, and is therefore used in this study to describe the nonlinear viscoelastic behaviour of a single ply. The constitutive equations for arbitrary loading conditions are expressed as

$$\varepsilon_i(t) = g_{ii}^{(0)}\big(\sigma_{eq}(t)\big)S_{ij}^{(0)}\sigma_j(t) + g_{ii}^{(1)}\big(\sigma_{eq}(t)\big) \times \int_{0^-}^{t} \Delta S_{ij}(\psi_{ij}(t) - \psi_{ij}(\tau))\frac{d}{d\tau}\left[g_{ii}^{(2)}\big(\sigma_{eq}(\tau)\big)\sigma_j(\tau)\right]d\tau \tag{5}$$

where there is no summation on i, and $i, j = 1, 2, 6$. In equation (5), $\varepsilon_i(t)$ is the time-dependent strain component, and the first term on the right-hand side represents the immediate elastic response. Similar to equation (4), the $g_{ii}^{()}$ terms are stress-dependent nonlinear parameters, which depend on

an effective stress $\sigma_{eq}(t)$, and $\sigma_j(t)$ is the applied stress component at time t. The second term on the right represents the convolution integral for a nonlinear viscoelastic model, where $\Delta S_{ij}(t)$ is usually represented as a Prony series; $\psi_{ij}(t)$ is the reduced time and is also stress dependent. The nonlinear ply-level parameters appearing in equation (5) are empirical in nature and are thus evaluated by fitting the model to available experimental data. It should be noted when $i=1$, equation (5) is reduced to a linear elastic equation since this corresponds to the ply fiber direction (i.e. $g_{11}^{(0)}=1$ and $g_{11}^{(1)}=g_{11}^{(2)}=0$).

Equations (4) and (5) are applicable for an orthotropic ply. In order to evaluate the viscoelastic behaviour of the laminate, an approach utilizing the framework of CLT is invoked in this study (Tuttle and Brinson, 1986). In brief, the creep strain of each ply is first determined based on the local driving ply stress, assuming independent deformation of each ply. Thereafter, time-dependent compliance matrix is determined for the whole laminate using CLT approach. A balance of forces and moments on the laminate yields the overall strain and an equivalent load for the laminate. The local driving stresses in individual plies are then re-evaluated to maintain uniform overall deformation in the laminate as a whole; this finally results into the constrained local ply strains. Overall, this approach predicts the variation of time-dependent strains in different plies of different orientations within a laminate, while accounting for the varying compliance changes and time-dependent constraining effects between plies.

Combined laminate viscoelasticity and damage evolution

The main goal of the current work is to develop a prediction model that combines the effects of microscopic ply crack evolution and nonlinear time-dependent behaviour for general multidirectional laminated composites in a coherent fashion. The novelty of the developed model is its ability to account for the influence of ply-level viscoelasticity and time-dependent damage evolution on the changing laminate stiffness (or, equivalently, compliance) during creep loading. These two effects have been superimposed in the prediction model, where it is assumed that the micro-cracks only affect the elastic response of the laminate and thus do not influence the viscoelastic laminate properties. As shown in the Results section, this approximation can be considered satisfactory for our purpose here. Therefore, the compliance tensor for the damaged laminate under creep is given by

$$S_{pq}^L(t, D) = S_{pq,\text{elastic}}^L(D) + S_{pq,\text{creep}}^L(t) \tag{6}$$

The first term on the right-hand side of equation (6) corresponds to the effective damaged laminate elastic compliance, which accounts for the effects of ply cracking and can be defined using equation (2). The second term in equation (6) is the laminate creep compliance. The first term is obtained using the results of the FE micromechanical computations, while the second term is obtained from the procedure described in the previous subsection along with the ply-level compliance defined by equation (4). As explained before, the laminate damage state is described by the time-varying crack density in each ply. When a laminate is subjected to creep loading, the ply CODs will also continue to increase with time, and thus the evolving creep strain will affect the energy release rate (see equation (3)). It should be noted that the CODs are also affected by the evolving crack density (i.e. due to crack shielding). Moreover, the far-field ply stress σ_2^α also changes with time due to the increasing laminate creep strain, which also directly affects W_I. Thus, although the effects of damage and viscoelasticity are superimposed in equation (6), the influence of time on damage evolution is in fact captured by the prediction model. Due to the inherently different nature of damage processes under elastic and viscoelastic conditions, it was determined that G_{Ic} shall be

described using a time-dependent function. This behaviour has been experimentally observed previously by Asadi (2013). An exponentially decaying formulation for critical energy release rate is used herein, i.e. $G_{Ic}(t) = G_{Ic}(0) \exp(-(t \cdot 10^{-10})^{0.105})$, where fitting constants were determined by calibrating the model with available experimental data. It should be noted that this time-dependent critical energy release rate holds for the particular ply material considered in this study and must be re-calibrated for other material systems. Also, $G_{Ic}(t)$ may in fact be dependent on the magnitude of the applied creep stress, which implies the fitting parameters are not constant; however, this is not known at this stage and therefore not considered here.

The total strain tensor for a damaged laminate under creep is given by

$$\varepsilon_p^L(t) = S_{pq,\text{elastic}}^L(D)\sigma_{CREEP,q}^L + \varepsilon_{CREEP,p}^L(t) \tag{7}$$
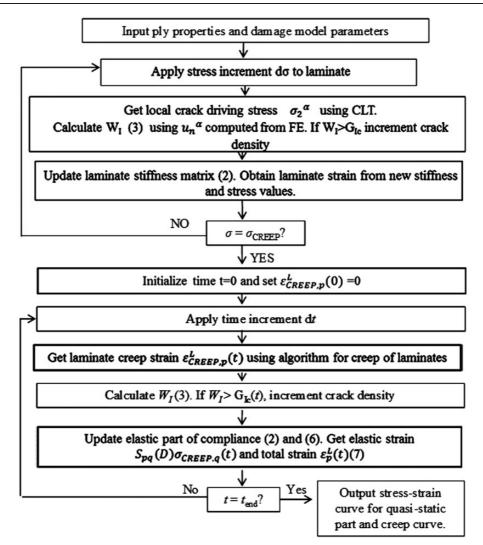
where the second term represents the creep strain for the laminate without damage, which is evaluated using the procedure outlined in the previous subsection along with ply-level strain evaluated using equation (5), while the first term represents the effect of damage on the laminate strain. Also, $S_{pq,\text{elastic}}^L(D)$ denotes the effective damaged laminate elastic compliance for a given damage state, $D(t)$, and $\sigma_{CREEP,q}^L$ represents the components of the applied creep stress tensor.

The overall procedure for the developed model is illustrated in the flowchart of Figure 3. It is notable that the model described here requires minimal experimental data, namely ply elastic and viscoelastic properties as well as laminate geometry. The first part of the code is a quasi-static ramp-up in stress that does not take viscoelastic properties into account, whereby during each iteration of the loop, the applied stress on the laminate is incremented. For each ply, the energy release rate W_I is calculated using equation (3), where the CODs are obtained from the micromechanical FE model for different crack densities, and the local ply crack opening stress σ_2^α is obtained using CLT. When W_I is larger than G_{Ic} in any of the laminate plies, the crack density is updated. Recall that the stochastic nature of ply cracking is accounted for by the model. From the calculated crack densities in all plies, the stiffness of the damaged laminate is updated using equation (2), which is subsequently used to evaluate the new laminate strain. The quasi-static loop ends when the applied stress at creep initiation is attained. The second part of the code simulates the effect of creep loading at a constant stress. During each iteration with a time step of 10^2 s, the increase in laminate creep strain is computed first under undamaged conditions, then for a progressively damaged laminate. To determine the creep strain increment due to damage, the energy release rate W_I is re-evaluated and compared to $G_{Ic}(t)$, where the crack density is updated whenever the crack multiplication criterion is met. The elastic stiffness matrix is then updated using equation (2), and the total laminate compliance is updated using equation (6). The updated laminate elastic strain component is added to the creep strain using equation (7) in order to obtain the total laminate strain. The procedure is repeated until a predetermined time is attained.

Results and discussion

Model validation

In order to validate the proposed multi-scale model, the predictions were verified with available experimental data for three different carbon fiber reinforced polymer (CFRP) laminates – two cross-ply laminates, namely $[0_3/90_3]_s$, and $[0/90_3]_s$, and a multidirectional laminate, $[\pm45/90_2]_s$. It is noted that experimental data on creep response of damaged laminates are very limited in the literature. First, we describe validation of the model for quasi-static case of a multidirectional laminate.
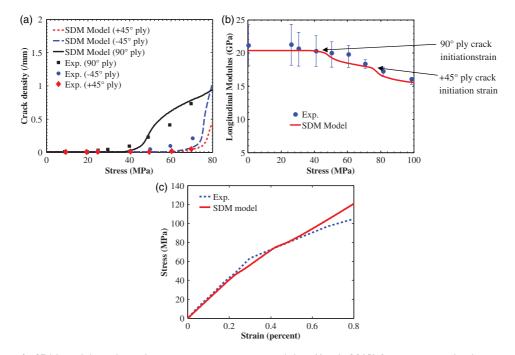
Figure 3. Flowchart illustrating the numerical procedure of the developed model, which was implemented into the MATLAB programming environment.

Multidirectional laminates undergoing cracking in multiple plies. Before investigating the effects of creep on damage evolution and performance degradation, the quasi-static response of the $[\pm 45/90_2]_s$ CFRP laminate is predicted and compared to the experimental test data reported by Asadi (2013). Equation (2) constitutes the basic constitutive model for the damaged laminate, where the evolution of ply cracking is predicted using the energy-based approach, see equation (3). The elastic properties for the carbon/epoxy plies are shown in Table 1.

The predicted and experimental crack density evolution data during quasi-static loading are shown in Figure 4(a). The ply cracks initiate in the $90°$ plies first, as expected, at about 40 MPa applied stress, consistent with experimental observations. Qualitatively, the overall trends in the evolution of crack densities in different plies agree well with the test data. Quantitatively, it is clear

Table 1. Elastic ply properties for the $[\pm45/90_2]_s$ CFRP laminate.

Material property	Value
E_1 (GPa)	113
E_2 (GPa)	9.68
G_{12} (GPa)	4.83
ν_{12}	0.3

Figure 4. SDM model results and comparison to experimental data (Asadi, 2013) for quasi-static loading on a $[\pm45/90_2]_s$ carbon-fibre/epoxy laminate: (a) crack density evolution in different plies; (b) stiffness degradation; (c) stress–strain curve. The SDM model used here does not include viscoelastic effects. SDM: synergistic damage mechanics.

that the model predictions are accurate for the 90° ply cracks, but less accurate for the 45° plies at higher applied stresses. In the study by Asadi (2013), experimental tests revealed that delamination was observed at applied stresses of 75 MPa. Since this mechanism of damage is not considered by the prediction model, which only takes into account sub-critical matrix micro-cracking, this deviation at higher stresses is expected. Nonetheless, the model is accurate at lower applied stresses, and since the creep simulations will be performed at approximately 50 MPa prior to the onset of delamination, this is deemed acceptable. The corresponding quasi-static axial stiffness degradation results are shown in Figure 4(b). Again, the predictions correlate well with the available experimental data, which are well within the error bars shown in the plot. The sudden changes in stiffness due to the onset of 90° ply cracks and 45° ply cracks are also clear. Figure 4(c) shows the predicted stress–strain

Table 2. Parameters for the nonlinear creep model described in equation (4), which were obtained using the experimental data in Asadi (2013).

S_{22} (transverse)		S_{66} (shear)	
$S_{22}^{(0)}$ (MPa^{-1})	1.033×10^{-4}	$S_{66}^{(0)}$ (MPa^{-1})	2.07×10^{-4}
$\triangle S_{22}$ (MPa^{-1})	0.002675	$\triangle S_{66}$ (MPa^{-1})	0.002113
τ_{22} (s)	3.49×10^{14}	τ_{66} (s)	1.52×10^{9}
c	0.2863	c	0.3638

response, which also shows good agreement with the experimental data. Figure 4 thus validates the developed model for multidirectional laminates during quasi-static loading.

Next, the deformational response of the $[\pm45/90_2]_s$ CFRP laminate under creep loading is predicted and compared to the experimental test data. The model parameters for ply creep compliance (see equation (4)) are provided in Table 2. It is notable that according to previous experimental studies, only the transverse and shear components of the ply compliance tensor were found to be time dependent. The non linear stress-dependent ply parameters are also obtained from the experimental data reported in Asadi (2013) and are defined as functions of temperature, T, by the following expressions

$$
\begin{aligned}
g_{22}^{(0)} &= 1.0414 \\
g_{22}^{(1)} &= 0.0414\sigma_2 + 1.0175 \\
g_{22}^{(2)} &= 0.001\sigma_2 T + 0.0143\sigma_2 + 0.0071T + 0.4391 \\
\alpha_{\sigma,22} &= 0.0003\sigma_2 T - 0.0308\sigma_2 - 0.0041T + 1.2134
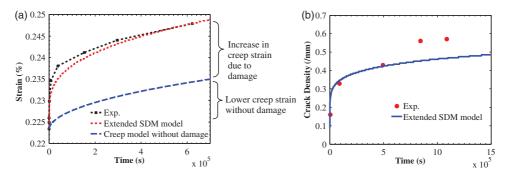\end{aligned}
\tag{8}
$$

$$
\begin{aligned}
g_{66}^{(0)} &= 0.005\sigma_6 + 0.9754 \\
g_{66}^{(1)} &= 0.0055\sigma_6 + 0.9774 \\
g_{66}^{(2)} &= 0.0018\sigma_6 T - 0.1342\sigma_6 - 0.0053T + 1.3044 \\
\alpha_{\sigma,66} &= 0.0002\sigma_6 T - 0.0502\sigma_6 - 0.0027T + 1.2676
\end{aligned}
\tag{9}
$$

Two simulations were conducted to predict the laminate creep strain evolution, the first without the effects of ply cracking (i.e. damage) and the second whereby the evolution of cracking was considered. The results for the laminate creep strain evolution under a constant creep stress of 45 MPa are shown in Figure 5(a) along with the experimental data. It can be seen that the inclusion of damage in the developed model significantly improves the predicted creep strain evolution, showing that damage is an important phenomenon affecting creep for these laminates. The corresponding predicted 90° ply crack density evolution is shown in Figure 5(b), along with the experimental data. The initial crack density at a stress of 45 MPa is accurately predicted at approximately 0.1 cracks/mm. The subsequent crack evolution prediction also correlates reasonably well with the experimental data and evolves somewhat similarly to the creep strain due to an apparent proportionality between creep strain and CODs and thus the crack density evolution. The crack density
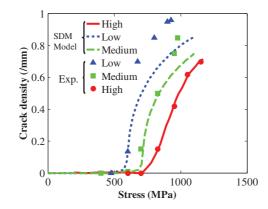
Figure 5. Results of the extended SDM model and comparison to experimental data (Asadi, 2013) for a $[\pm45/90_2]_s$ laminate subjected to a constant creep stress of 45 MPa: (a) laminate creep strain evolution and (b) 90° ply crack evolution. Note that the initial experimental creep strain at time $t = 0$ s was adjusted so that the predicted results and the experimental data coincided at the onset of creep. SDM: synergistic damage mechanics.
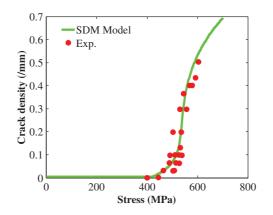
at longer times is determined to approach a saturation value of 0.5 cracks/mm, which is slightly lower than the experimental data.

As depicted above, using the ply elastic and viscoelastic properties along with the critical energy release rate, the developed model can predict strain and damage evolutions reasonably well. Minor discrepancies between predictions and test data can be attributed to inherently different nature of damage processes under quasi-static and viscoelastic conditions, which the current model may not capture fully. For instance, the crack density is well estimated up until 6×10^5 s, whereas the crack density is slightly under-predicted beyond this time range. Nonetheless, the lack of experimental creep data beyond 10^6 s precludes a direct comparison with the model predictions. It should be noted, however, that viscoplasticity may cause supplementary strains at long times, which are not currently accounted for by the prediction model. Moreover, the model assumes damage only affects the elastic properties of the laminate and not its viscoelastic time-dependent compliance. As shown by Varna et al., (2004) matrix cracks will cause degradation in time-dependent stiffness, so that accounting for this effect may aid in improving the results. Future work should consider all these effects to improve the accuracy of the model.

Cross-ply laminates undergoing cracking in transverse plies. In order to showcase the versatility of the model, the quasi-static response of a $[0_3/90_3]_s$ cross-ply laminate is also evaluated because it has different thickness ratios of cracking and non-cracking plies, and the test data are from a different source (Nguyen and Gamby (2007). Although the experimental data revealed that the laminate exhibited little time-dependent response, it was stated in the study that the crack density evolution under quasi-static was dependent on the applied strain rate. In order to account for the variation in crack density evolution at different applied strain rates for our predictions, the critical energy release rate G_{Ic} was defined to be a function of the applied strain rate based on data provided in the cited study. The predicted and experimental results are shown in Figure 6, which demonstrates that the current model accurately predicts crack initiation at lower stresses for lower applied loading rates, which is expected. It can also be seen that at high loading rates, when time-dependent effects are minimal, the prediction model is very accurate. As the loading rate is decreased by a factor of 100, the model predictions are less accurate at higher applied stresses as shown in Figure 6. This is most likely due to the fact that time-dependent effects were neglected for the quasi-static simulations.

Figure 6. Predicted crack density evolution for a $[0_3/90_3]_s$ cross-ply laminate under quasi-static loading at different levels of strain rate (low, medium and high), along with experimental data from Nguyen and Gamby (2007).

Figure 7. Predicted and experimental (Ogi and Takao, 1999) 90° ply crack density evolution during quasi-static loading for a $[0/90_3]_s$ cross-ply laminate; the prediction assumes no viscoelastic effects.

It is expected that at very lower applied strain rates, the laminate will exhibit some creep behaviour due to the increased loading time, which will drive crack multiplication slightly higher.

In order to provide further validation for the current model, our predictions will be compared to the available experimental results of Ogi and Takao (1999) for a $[0/90_3]_s$ CFRP cross-ply laminate. A quasi-static simulation was first performed using the elastic ply properties presented in Table 1, where the predicted and experimental crack density evolution results are shown in Figure 7. A good agreement between the model predictions and the test data is shown. The accuracy of the results suggests that time-dependent effects were not important during loading due to the relatively high applied strain rate.

The creep model presented in the previous section is now applied for the $[0/90_3]_s$ CFRP laminate, where the ply transverse creep properties were determined by fitting the unidirectional ply creep curves provided in Ogi and Takao (1999) with equation (4) at an applied stress of 510 MPa. It was assumed that all nonlinear parameters were equal to 1 in this instance because there were not sufficient data in the cited source to determine them precisely. This implies that the nonlinear

Table 3. Parameters used for the creep compliance model, equation (4), as obtained by fitting the experimental creep curve for 90° unidirectional plies, at a stress level of 510 MPa.

S_{22} (transverse)	
ΔS_{22} (MPa^{-1})	9.80×10^{-7}
τ_{22} (s)	319

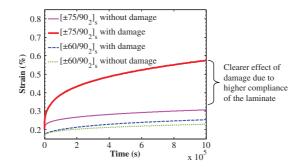Source: Reproduced with permission from Ogi and Takao (1999).

Figure 8. Predicted and experimental (Ogi and Takao, 1999) results for a [0/90$_3$]$_s$ cross-ply laminate subjected to a constant creep stress of 530 MPa: (a) 90° ply crack density evolution and (b) corresponding laminate creep strain.

parameters are stress independent and thus, the current analysis is only valid for stresses close to 510 MPa. Since the magnitude of creep stress we consider is 530 MPa, this is deemed acceptable. The creep parameters obtained through data fitting are presented in Table 3, where a time constant of 10^9 s was used to evaluate $G_{Ic}(t)$. It should be noted that the magnitude of the ΔS_{22} value presented in Table 3 is notably lower compared with the values shown in Table 2, which is a result of forcing the nonlinear parameters to be stress independent. The predicted and experimental crack density evolution and laminate creep strain results are shown in Figure 8(a) and (b), respectively, for a constant applied creep stress of 530 MPa. From Figure 8(a), it is clear that the crack density evolution in the 90° ply correlates well with the experimental data when $t > 2 \times 10^5$ s, but is slightly under-predicted during the early stages of creep. From Figure 8(b), it can be seen that including the effect of damage evolution on the elastic properties greatly enhances the accuracy of the predicted laminate creep strain. The laminate creep strain at longer times is slightly underestimated by the prediction model and is possibly due to neglected viscoplastic strains.

Predictions for [±60/90$_2$]$_s$ and [±75/90$_2$]$_s$ CFRP laminates

In order to showcase the predictive capabilities of the developed model for general multidirectional laminates, the results for two additional CFRP laminates, namely [±60/90$_2$]$_s$ and [±75/90$_2$]$_s$, are analyzed here. It should be noted that no supplementary data were required to make these predictions. The elastic and time-dependent ply properties were given in Tables 1 and 2 and by equations
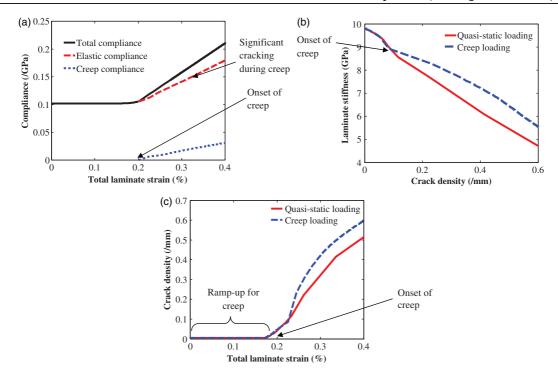
Figure 9. Predicted creep strain evolution for $[\pm60/90_2]_s$ and $[\pm75/90_2]_s$ CFRP laminates, with and without the effects of damage, subjected to a constant creep stress of 19 MPa.
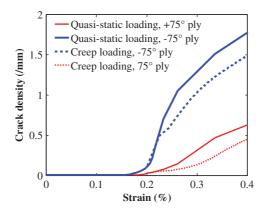
(8) and (9). Two creep simulations were performed for two different constant stresses of 16 MPa and 19 MPa, respectively, using the developed MATLAB algorithm (see Figure 3).

The creep strain results for the two laminates studied are shown in Figure 9. Since the $[\pm75/90_2]_s$ is more compliant in the loading direction, the initial strain at time $t = 0$ s for a constant creep stress of 19 MPa is notably higher compared to the $[\pm60/90_2]_s$ laminate, which is expected. The effect of damage on the predicted creep strain is also more noticeable for the $[\pm75/90_2]_s$ laminate – the $[\pm60/90_2]_s$ laminate did not exhibit any significant damage evolution (see Figure 9). The strain increases by approximately 0.10% for the $[\pm75/90_2]_s$ laminate when damage is not considered, whereas the increase is approximately 0.38% when the effects of damage are considered. This is due to two main factors. First, the ply crack driving stresses, σ_2^α, from equation (3) are higher for the more compliant $[\pm75/90_2]_s$ laminate, which undergoes greater laminate strains in the loading direction. Thus, as the laminate creep strain continues to increase, the energy release rate W_I increases by a greater magnitude, which favours crack multiplication in both the 90° and 75° plies. For the $[\pm60/90_2]_s$ laminate, the laminate creep strain increases by a lower magnitude, and thus, its effects on crack multiplication in the 90° and 60° plies is minimal. This same effect can also be seen in Figure 5 for the $[\pm45/90_2]_s$ laminate since the crack density evolution in the 90° ply has a similar shape to the creep strain curve; it should be noted that the applied loading for the $[\pm45/90_2]_s$ laminate was greater at 45 MPa. Second, since the critical energy release rate G_{Ic} is an exponentially decreasing function of time, for the $[\pm75/90_2]_s$ laminate, it directly enhanced the crack multiplication process due to the adequate laminate strain magnitudes. For the $[\pm60/90_2]_s$ laminate, the laminate creep strain magnitudes were not sufficiently high to promote damage even though G_{Ic} decreased with time.

Figure 10(a), (b) and (c), respectively, show for the $[\pm75/90_2]_s$ laminate the evolution of compliance with laminate strain, the evolution of longitudinal stiffness with crack density, and the evolution of crack density in the 90° ply. From Figure 10(a), we can see that there is no notable change in the compliance before approximately 0.20% strain, which corresponds to the start of the creep portion of the simulation. The evolution of crack density, and thus elastic compliance, is minimal during the quasi-static portion, which is due to the relatively small applied stress of 19 MPa. After the onset of creep, the elastic compliance increases by 0.075 GPa^{-1} during the duration of creep loading (up to 0.4% strain), which is a result of notable crack evolution in the 90° ply. The time-dependent creep compliance increases by 0.02 GPa^{-1} during the same creep interval, which is approximately a quarter of the increase in the elastic compliance. This shows that the influence of ply crack evolution during creep loading in the studied laminates is significant and is a result of the specific layup considered. From Figure 10(b), we can see that laminate stiffness, which is affected by
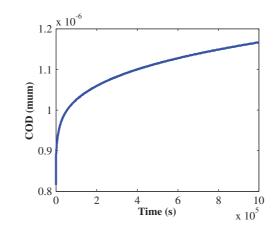
Figure 10. Predicted results for the $[\pm75/90_2]_s$ laminate under a creep stress of 19 MPa: (a) evolution of different components of compliance (creep and elastic), (b) evolution of stiffness with 90° ply crack density and (c) evolution of 90° ply crack density for creep and quasi-static loading.

Figure 11. Predicted off-axis ply crack density evolution for a $[\pm75/90_2]_s$ laminate under creep at 19 MPa and quasi-static loading. The plots show that cracks evolve slower during creep loading at low strain levels.

the crack density evolution in all plies, decreases linearly during the initial stages of creep. It should be noted that during creep loading, the $\pm75°$ ply crack density is less advanced when compared to a quasi-static loading case, as is shown in Figure 11. Therefore, stiffness degradation is greater for the quasi-static case when compared to creep loading (see Figure 10(b)).
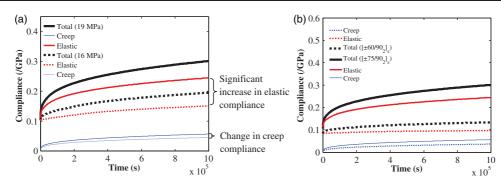
Figure 12. Predicted COD evolution for the $90°$ ply in a $[\pm 75/90_2]_s$ laminate undergoing creep at 19 MPa, showing a clear increase linked to creep strain evolution. The increase in COD affects crack density evolution through its effect on the energy release rate W_l.

From Figure 10(c), we can see that crack density evolution in the $90°$ ply during the load ramp-up is minor, and that it increases significantly during creep loading. The crack density under creep at a specific strain magnitude is greater when compared to the quasi-static loading case (see Figure 10(c)), which is a result of time-dependent effects in the thicker $90°$ ply. This is manifested through the critical energy release rate and ply CODs, which enhance ply crack multiplication. An increase in crack density tends to decrease COD for elastic laminates (Montesano and Singh, 2015a); however, in the $90°$ ply the COD increases (see Figure 12), which is a result of increasing creep strain. This demonstrates that the time-dependent effect on the $90°$ ply COD is notable for the laminates studied, which is an important result in this study. Furthermore, it can be seen from Figure 10(c) that the crack density begins to plateau at higher strains; however, the characteristic damage state (CDS) is not reached before the end of the creep test. This plateau is due to the fact that the creep strain also reaches a plateau after a notable time increment, which limits the crack driving stresses during the latter stages of creep loading.

Figure 13(a) shows the evolution of laminate axial compliance for two different stress levels during creep loading of a $[\pm 75/90_2]_s$ laminate. It can be seen that there is a small increase in the creep compliance component when the stress is increased from 16 MPa to 19 MPa. This is due to the nonlinearity in the KWW creep model (see equation (4)), which accounts for a higher compliance at higher stresses through the nonlinear parameters defined in equations (8) and (9). On the other hand, the elastic compliance at the 16 MPa applied stress increases from $0.1\,GPa^{-1}$ to $0.2\,GPa^{-1}$ during creep, whereas it increases from $0.1\,GPa^{-1}$ to $0.3\,GPa^{-1}$ at the 19 MPa applied stress. This is due to enhanced crack evolution at the 19 MPa applied stress level, leading to a greater effect on stiffness degradation. Once again it is demonstrated that ply crack evolution directly influences the long-term laminate response. It can be inferred from Figure 13 that ply cracking leads to a significant increase in total laminate compliance, even over narrow stress ranges.

Figure 13(b) shows the different components of the compliance (creep and elastic) for the $[\pm 60/90_2]_s$ and $[\pm 75/90_2]_s$ laminates at the same stress level of 19 MPa. The creep compliance of the $[\pm 60/90_2]_s$ laminate is approximately half that of the $[\pm 75/90_2]_s$ laminate. This is due to the difference in the stacking sequence and points to the importance of an accurate creep model that considers

Figure 13. (a) Predicted evolution of the elastic and time-dependent (creep) components of the $[\pm 75/90_2]_s$ laminate compliance, at two different stress levels, demonstrating the impact of damage on compliance increase. (b) Predicted evolution of the different components (creep and elastic) of compliance for the two different laminates, at a stress of 19 MPa.

deformation in both the shear and transverse directions. The elastic compliance is also much lower for the $[\pm 60/90_2]_s$ and evolves very little due to the decreased amount of ply cracking, which is a result of lower energy release rates caused by lower laminate creep strains.

Conclusions

This paper presented a physics-based multi-scale model to predict the simultaneous ply crack evolution and time-dependent deformational response of general multidirectional laminates subjected to quasi-static and creep loads. The model follows the framework of SDM and utilizes computational micromechanics to define the corresponding damaged laminate stiffness degradation parameters, requiring only ply-level elastic and viscoelastic empirical data as input. The critical energy release rates associated with ply crack multiplication are also evaluated computationally through a crack closure concept. A nonlinear viscoelastic Schapery-type model is used to represent the ply behaviour, which is cast into the framework of CLT for predicting the total laminate time-dependent response. The effects of time-dependent behaviour and damage evolution are superimposed to evaluate the laminate compliance and the corresponding creep strains for various cross-ply and multidirectional laminates. Model predictions for the studied laminates subjected to quasi-static and creep loading correlated well with available experimental data, with respect to the evolution of ply crack density and laminate creep strain. The predictive capabilities of the model were further shown through a parametric evaluation of $[\pm\theta/90_2]_s$ laminates subjected to creep loading at various applied stresses. The developed model is the first reported model that considers the effects of viscoelasticity, ply crack evolution and stiffness degradation for general multidirectional laminates simultaneously and will provide an effective means to assess the long-term durability of structures made from these laminates. The future model development should focus on a careful investigation of the interactive effects between time-dependent damage evolution and creep deformation response, as well as the affect of viscoplastic strains on multidirectional laminates.

Declaration of Conflicting Interests

Funding

References

Ahci E and Talreja R (2006) Characterization of viscoelasticity and damage in high temperature polymer matrix composites. *Composite Sciencesand Technology* 66: 2506–2519.

Asadi A (2013) *A model for time-independent and time-dependent damage evolution and their influence on creep of multidirectional polymer composite laminates*. PhD Thesis, University of Manitoba, Canada.

Asadi A and Raghavan J (2011) Influence of time-dependent damage on creep of multidirectional polymer composite laminates. *Composites Part B* 42: 489–498.

Hashin Z (1987) Analysis of orthogonally cracked laminates under tension. *Journal of Applied Mechanics* 54: 872–879.

Lévesque M, Derrien K, Baptiste D, et al. (2008) On the development and parameter identification of Schapery-type constitutive theories. *Mechanics of Time-dependent Materials* 12: 95–127.

Lim SG and Hong CS (1989) Prediction of transverse cracking and stiffness reduction in cross-ply laminated composites. *Journal of Composite Materials* 23: 695–712.

Montesano J and Singh CV (2015a) A synergistic damage mechanics based multiscale model for composite laminates subjected to multiaxial strains. *Mechanics of Materials* 83: 72–89.

Montesano J and Singh CV (2015b) Predicting evolution of ply cracks in composite laminates subjected to biaxial loading. *Composites Part B* 75: 264–273.

Montesano J and Singh CV (2015c) Critical stiffness damage envelopes for multidirectional laminated structures under multiaxial loading conditions. Under review.

Nguyen T and Gamby D (2007) Effects of non-linear viscoelastic behaviour and loading rate on transverse cracking in CFRP laminates. *Composites Science and Technology* 67: 438–452.

Ogi K and Takao Y (1999) Evolution of transverse cracking in CF/Epoxy cross-ply laminates under creep loading. *Journal of Reinforced Plastics and Composites* 18: 1220–1230.

Rozite L, Varna J, Joffe R, et al. (2011) Characterization and modeling of performance of polymer composites reinforced with highly non-linear cellulosic fibers. In: *IOP conference series: Materials science and engineering*, Nancy, France, 7–8 November, Vol. 31.

Schapery RA (1969) On the characterization of nonlinear viscoelastic materials. *Polymer Engineering and Science* 54: 295–310.

Singh CV and Talreja R (2008) Analysis of multiple off-axis ply cracks in composite laminates. *International Journal of Solids and Structures* 45: 4574–4589.

Singh CV and Talreja R (2009) A synergistic damage mechanics approach for composite laminates with matrix cracks in multiple orientations. *Mechanics of Materials* 41: 954–968.

Singh CV and Talreja R (2010) Evolution of ply cracks in multidirectional composite laminates. *International Journal of Solids and Structures* 47: 1338–1349.

Talreja R (1985) Transverse cracking and stiffness reduction in composite laminates. *Journal of Composite Materials* 19: 355–375.

Talreja R (1994) Damage characterization by internal variables. In: Talreja R (ed.) *Damage Mechanics of Composite Materials*. Amsterdam, the Netherlands: Elsevier, pp. 53–78.

Talreja R and Singh CV (2012) *Damage and Failure of Composite Materials*. Cambridge, UK: Cambridge University Press.

Tuttle ME and Brinson HF (1986) Prediction of long-term creep compliance of general composite laminates. *Experimental Mechanics* 26: 89–102.

Varna J, Krasnikovs A, Kumar RS, et al. (2004) A synergistic damage mechanics approach to viscoelastic response of cracked cross-ply laminates. *International Journal of Damage Mechanics* 13: 301–334.